Available online at www.sciencedirect.com
SCIENCE @ DIRECT®

Review of Palaeobotany and Palynology 128 (2004) 55–79

Review of Palaeobotany & Palynology

www.elsevier.com/locate/revpalbo

Comparison of the Holocene and Eemian palaeoenvironments in the South Icelandic Basin: dinoflagellate cysts as proxies for the North Atlantic surface circulation

F. Eynaud*, J.L. Turon, J. Duprat

Département Géologie et Océanographie, UMR–CNRS 'EPOC' 5805, Université Bordeaux I, Avenue des Facultés,
33405 Talence, France

Abstract

A precise assessment of the hydrological changes in the northern Atlantic Ocean throughout the last climatic cycle stands as one of the key priorities for understanding the mechanisms of global climate change. A high resolution micropalaeontological study of a sediment core (MD95-2015) retrieved from the South Icelandic Basin, allows us to infer patterns of North Atlantic surface hydrological changes during the present (Holocene) and the ultimate (Marine Isotopic Stage 5) Interglacial periods. The downcore distribution of organic-walled dinoflagellate cysts (dinocysts) is used, in conjunction with additional proxies (sediment magnetic susceptibility, $CaCO_3$, stables isotopes and planktic foraminifer assemblages) to identify climatic instabilities of various amplitudes. These events are mostly characterised by prominent changes in relative abundance of the dinocysts *Spiniferites mirabilis* and *Operculodinium centrocarpum*, whose maximum values are thought to trace sea-surface temperature peaks at the core site. Two hypsithermal periods are identified on this basis, between 126 and 120 kyr BP and from 9.2 to 5.7 cal kyr BP (~8–5 ^{14}C kyr BP), respectively. Some discrepancies between the micropalaeontological tracers used are discussed here in the light of their qualitative and quantitative (transfer functions) ecological interpretation.

Keywords: dinoflagellate cyst (dinocyst); palaeoclimatology; Marine Isotopic Stage 5; Holocene; Eemian

1. Introduction

Over the last few decades, an increased awareness of anthropological impacts on climate has lead to greater study of natural climatic variability. An important aspect of this research concerns the study of past and sub-recent climatic proxies derived from marine sequences. The 'IMAGES programme' is a global research network (http://images.pclab.ifg.uni-kiel.de/start.html) that aims to collect high quality and high resolution oceanic sedimentary records and multiproxy data (Cortijo et al., 2000). Core MD95-2015, located in the South Icelandic Basin and discussed in the present paper, was collected during the first IMAGES coring cruise (Bassinot and Labeyrie, 1996). This core displays very high sedimentation rates during interglacial stages (Giraudeau et al., 2000) and organic-walled dinoflagellate cysts (dinocysts) have been investigated from these time intervals.

---

* Corresponding author. Tel.: +33-540-003319; Fax: +33-540-000848.

E-mail addresses: eynaud@geocean.u-bordeaux.fr (F. Eynaud), turon@geocean.u-bordeaux.f (J.L. Turon), j.duprat@geocean.u-bordeaux.fr (J. Duprat).

0034-6667/03/$ – see front matter © 2003 Elsevier B.V. All rights reserved.
doi:10.1016/S0034-6667(03)00112-X

The interglacial periods of the Quaternary offer direct analogues for the present interglacial (Holocene). Evaluation of their climatic evolution and transition to glacial periods could therefore offer insights into the natural evolution of our modern climate. Until now, the Last Interglacial Period, corresponding to the Marine Isotopic Substage 5e (MIS 5e) has been the most extensively studied. However, it has been shown recently that Marine Isotopic Stage 11 is a better analogue with specific regard to orbital forcing (e.g. Poore and Dowsett, 2001; Forsstrom, 2001; Loutre and Berger, 2003). Interest about MIS 5e was boosted at the beginning of the last decade, when the Grip Ice Core record revealed large climatic variations during this supposed stable Last Interglacial Period (GRIP members, 1993). Many authors confirmed this result thereafter, specifically in continental sequences (e.g. Thouveny et al., 1994) but no similarly high variability was observed in the marine records (e.g. Cortijo et al., 1994). The debate was, however, rapidly closed when it was shown that the ice record was disturbed by stratigraphic distortions (Johnsen et al., 1995). At present, a crucial question animates the palaeoclimatic discussions about MIS 5e: the question of its length (e.g. Sanchez-Goñi et al., 1999; Kukla et al., 2002; Shackleton et al., 2002). Recent work (Shackleton et al., 2002) suggests that MIS 5e extends from 132 to 115 ka BP and is substantially different to the Eemian period, which people erroneously consider to be the equivalent of MIS 5e (the same confusion is made regarding MIS 1 and the Holocene – see Sánchez-Goñi et al., 2000 for a review).

In this paper, we present data, obtained on MIS 5 (including MIS 5e) and on the last 13 cal kyr BP of MIS 1 from core MD95-2015, using dinocysts as a proxy for sea-surface palaeoenvironments of the South Icelandic Basin. Actually, the use of dinocysts as a potential sea-surface tracer has already been demonstrated throughout several studies in the North Atlantic Ocean (e.g. Williams, 1971; Wall et al., 1977; Turon, 1981; de Vernal et al., 1993, 1997, 2001; Harland and Howe, 1995; Matthiessen, 1995; Dale, 1996; Rochon et al., 1998, 1999; Eynaud et al., 2000, 2002; Boessenkool et al., 2001; Matthiessen and Knies, 2001). In addition, our study presents new data that contribute to document dinocyst ecology and climatostratigraphy in an oceanic sector that until now has been poorly investigated. A focus is made on two species, *Spiniferites mirabilis* and *Operculodinium centrocarpum*, which are affected by significant abundance changes throughout the core. These changes are discussed in the light of other proxy data available, to better discriminate between forcing parameters of the palaeoclimatic evolution. A comparison of dinocyst quantitative reconstructions vs. foraminiferal data is made on the Holocene period, to discuss the interpretation of the respective tracers.

2. Material and environmental setting

The investigated core MD95-2015 (58°46′N; 25°57′N; 2630 m water depth), is a giant Calypso core (34.42 m length) retrieved from the Gardar Drift (Fig. 1), a major contourite accumulation (Faugères et al., 1993, 1999). The Gardar Drift has been built by the deep-overflow of the eastern branch of North Atlantic Deep Water which southerly crosses the Iceland–Faeroe Ridge (Tomczak and Godfrey, 1994). The direct impact of this deep hydrodynamical configuration is shown by the sedimentological characteristics of core MD95-2015. Silt-sized sediments are preferentially accumulated on the drift, with a mainly Icelandic origin for terrigeneous material (Revel et al., 1996). Biogenic pelagic sediments are also redistributed along the drift. Nevertheless, the information given by the species composition of silt-sized microfossils (among them are dinocysts (Dale, 1976) but also foraminifera) is supposed to efficiently document the conditions of surface waters, at least on a regional scale, for the Holocene (Giraudeau et al., 2000). The Last Interglacial Period (MIS 5e), the most recent analogue of the Holocene, is also thought to have preserved surface water information in the same way.

Core MD95-2015 is located under the path of a major return current of the North Atlantic Drift (NAD): the Irminger Current (IC; Fig. 1). The IC flows westward from 50°N where the NAD divergence is observed (separating into the Norwegian

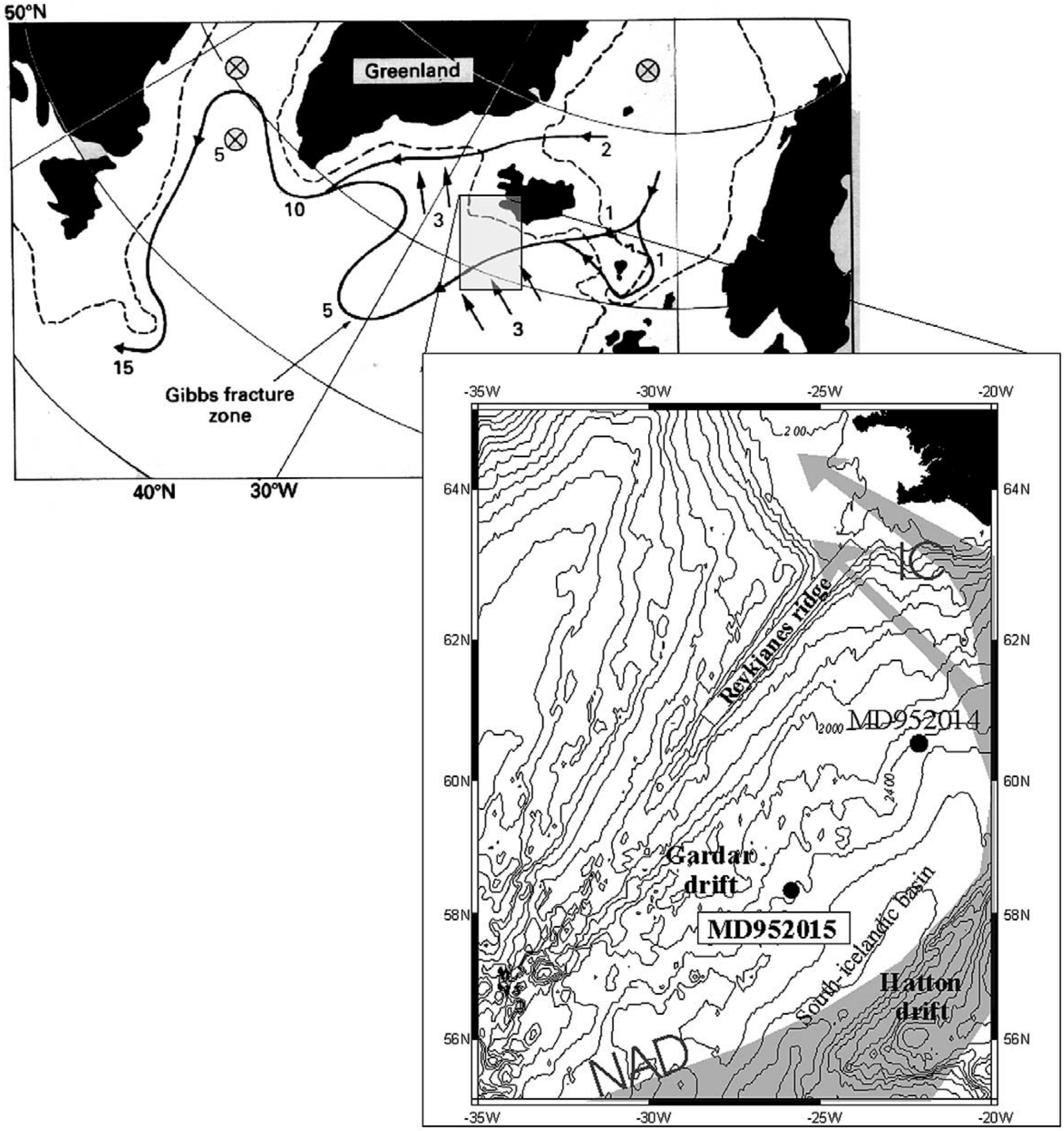

Fig. 1. Location of the studied core MD95-2015 with regard to its bathymetric position on the Gardar Drift and its position vs. the IC (grey arrow). The upper map shows the regional deep circulation pattern (major currents and their transport efficiency in Sv, after Tomczak and Godfrey, 1994). Core MD952014 mentioned in the text is also depicted on the Gardar Drift.

Coastal Current and the IC). At the latitude of the Icelandic Basin, the IC waters retain the biochemical properties of the warm and saline NAD, which in itself is primarily derived from the Gulf Stream. This is also evidenced by dinocyst distribution in surface sediments, as cysts of the species *Operculodinium centrocarpum*, assumed to thrive into NAD waters (Williams, 1971; Turon, 1978, 1981, 1984; Harland, 1983; Dale, 1996) are found in high quantity under the path of the IC (Rochon et al., 1999). Still with regards to dinocyst ecology, the MD95-2015 site is all the more interesting, because located at the northern limit of the present-day distribution area of the species *Spiniferites mirabilis* (Fig. 4a), the second cyst species with *O. centrocarpum*, that presents a characteristic downcore distribution.

The strategic position of core MD95-2015 in relation to the hydrological regional pattern, permits the observation of major and minor environmental changes related to fluctuations in global climate and thermohaline circulation. High sedimentation rates that characterise interglacial stages in this region (Giraudeau et al., 2000) furthermore allow high resolution palaeoclimatic studies.

3. Methods

3.1. Stratigraphy

The age model developed for the Holocene section of core MD95-2015 is based on linear interpolation of 12 AMS radiocarbon dates (Table 1). All the ^{14}C ages (^{14}C yr BP) have been converted to calendar ages (cal yr BP) using the CALIB programme version 4.1 (Stuiver et al., 1998) taking into account an age reservoir of 400 ^{14}C yr. Considering the work of Eiríksson et al. (2000) and Knudsen and Eiriksson (2002), a standard marine reservoir correction of 400 ^{14}C yr appears to be reasonable, at least on this southern sector of Iceland. In fact, these authors have shown for the last 4000 cal yr, that a 800 ^{14}C yr reservoir age correction should be applied to the northern Icelandic margin. They recommend a 400 ^{14}C yr correction however for periods that were highly influenced by the IC in the northern sector. The use of this standard marine reservoir correction is therefore justified in the construction of the MD95-2015 age model since the core is located just under the path of the IC. Sedimentation rates calculated on the basis of the age model vary from 21 cm/cal kyr up to 193 cm/cal kyr.

The stratigraphy of the MIS 5 section has been

Table 1
MD95-2015 age models for the interglacial sections

Holocene section

Depth (cm)	Age ^{14}C BP (yr)(−400 yr res. cor.)	Error (±)	Sedimentation rate (cm/1000 ^{14}C yr)	Age cal BP (yr)	Sedimentation rate (cm/cal kyr)
10	950	60	57.5	907	54.9
60	1 820	60	42.7	1 818	34.7
110	2 990	60	70.9	3 258	56.5
200	4 260	70	61.5	4 850	49.9
240	4 910	80	58.3	5 651	56.0
370	7 140	90	68.6	7 972	68.7
440	8 160	80	214.3	8 991	137.6
500	8 440	90	142.9	9 427	116.6
600	9 140	90	250.0	10 285	193.1
700	9 540	90	29.7	10 803	21.0
749	11 190	90	60.3	13 131	78.9
790	11 870	100			

MIS 5 section

Depth (cm)	Age (yr)	Sedimentation rate (cm/kyr)
1415	73 200	11.2
1530	83 500	8.5
1670	100 000	5.6
1740	112 500	17.9
2150	135 340	

AMS ^{14}C dates have been obtained on monospecific samples of the planktonic foraminifer *Globigerina bulloides* at the Laboratoire des Sciences du Climat et de l'Environnement, Gif-sur-Yvette, France (LSCE).

primarily established on the basis of the planktonic (*Globigerina bulloides*) and benthic (*Cibicides wuellerstorfi*) δ^{18}O measurements, the carbonate contents ($CaCO_3$ percentage of the bulk sediment) and the magnetic susceptibility data (Fig. 2). For the base of MIS 5, age-control points (Table 1) are deduced from a graphic comparison between the SPECMAP δ^{18}O composite curve and the δ^{18}O data (benthic and planktonic) from MD95-2015 (Fig. 2). Full-marine interglacial conditions (Last Interglacial Period = MIS 5e) are considered to have lasted only during the benthic isotopic plateau (Cortijo et al., 1999). The ages given for the isotopic heavy peak (200 years before the 6.2 event), the inflection point following the 5e plateau and the mid 5.3 event have been used as tie-points and their ages conform to Martinson et al. (1987), at respectively 135 340 yr, 112 500 yr and 100 000 yr.

As benthic δ^{18}O measurements were not available for the upper part of the MIS 5 section, age-control points for this period have been chosen on the basis of the carbonate contents (% $CaCO_3$) and the magnetic susceptibility data compared with the Greenland Ice-Sheet Project 2 (GISP2) δ^{18}O data (Grootes et al., 1993). Kissel et al. (1998, 1999) and Stoner et al. (2002) have shown that Magnetic Susceptibility (MS) on proximal cores can be tied to ice-core stratigraphies through regional climatic tie-points. The MS record of core MD95-2015 displays significant variations that are inversely correlated with peaks in $CaCO_3$ content (Fig. 2). Maximal $CaCO_3$ contents in Atlantic sediments are classically attributed to warm/interglacial conditions (an opposite pattern is found in Pacific sediments; Karlin et al. (1992)); it has therefore been inferred that peaks in $CaCO_3$ (correlated to low values of MS) correspond to Interstadial Events (IE) in Greenland. IE 21 and IE 23, as detected in the GISP2 δ^{18}O record (Grootes et al., 1993; Meese et al., 1994; Steig et al., 1994; Stuiver et al., 1995; Grootes and Stuiver, 1997), were therefore used as age-control points (Table 1; Fig. 2). A third tie-point

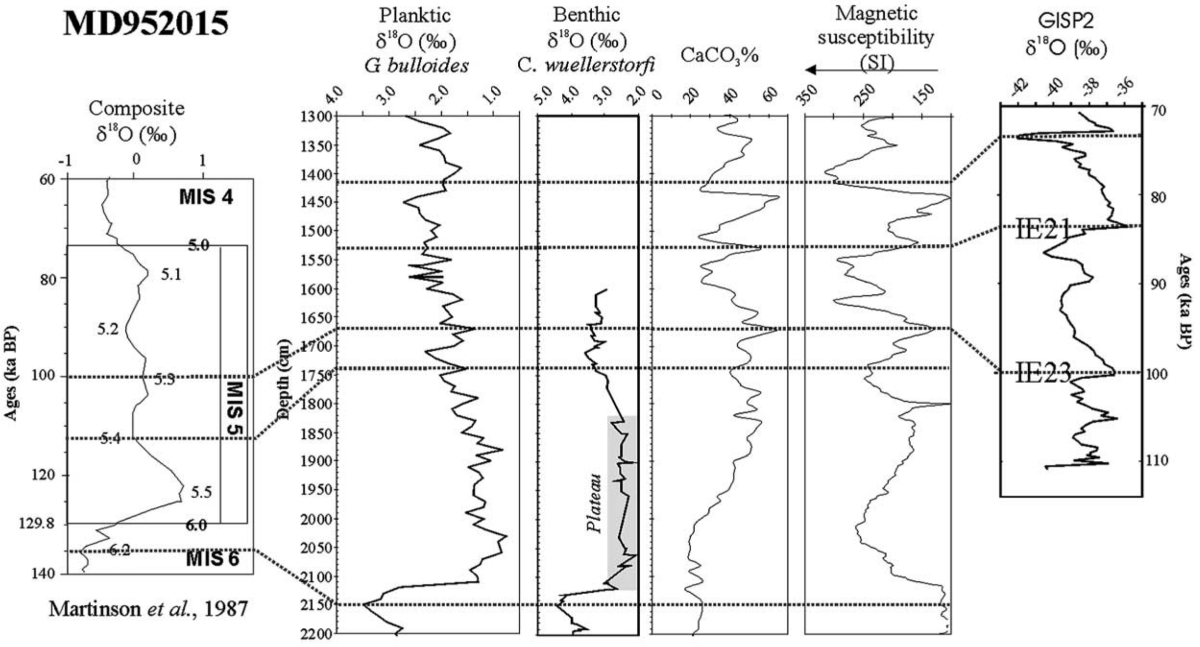

Fig. 2. MD95-2015 data (planktonic and benthic δ^{18}O, % $CaCO_3$, magnetic susceptibility) used for the construction of the age model (see also Table 1) for the Marine Isotopic Stage 5 section. Comparison with the SPECMAP stacked δ^{18}O curve (Martinson et al., 1987) and the GISP2 δ^{18}O data (Grootes et al., 1993; Meese et al., 1994) is shown. Interstadial events 21 and 23 (IE21 and IE23) are positioned according to Grootes et al. (1993).

was used in considering the minimum values of $\delta^{18}O$ from GISP2 (72 500 yr BP) that would inversely correspond to the maximum MS values recorded in this section of core MD95-2015 (1415 cm). The age model was constructed by linear interpolation between the five dated points. Validation of the MIS 5 age model for core MD95-2015 was independently obtained by comparison with data from the proximal core MD95-2014 (planktonic and benthic $\delta^{18}O$, % $CaCO_3$, magnetic susceptibility and dinocyst data). In core MD95-2014 isotopic stages and substages were clearly identifiable from $\delta^{18}O$ measurements alone (Eynaud, 1999).

3.2. Dinocyst analysis

Dinocyst analyses (111 samples) were performed on the < 150-μm sediment fraction at a median sampling resolution (every 10–20 cm), resulting in an age resolution from one sample per 100 yr to one sample per 1000 yr. Samples were prepared in accordance with de Vernal et al. (1996). Dinocysts were counted using a Zeiss Axioscope light microscope at ×400 magnification; an average of 300 dinoflagellate cysts were identified and examined from each sample. *Brigantedinium* specimens were grouped together because of uncertain species determination due to folding of the dinocysts: this concerns specimens of round, brown cysts such as *Brigantedinium simplex* and *Brigantedinium cariacoense* (the latter species is referenced also as *Protoperidinium* species for thecal name; see Zonneveld (1995)). Dinocyst assemblages were described by the respective percentages of each species, calculated on the basis of the total dinocyst sum including unidentified taxa and excluding reworked specimens. Dinocyst concentrations were calculated using the marker grain method (de Vernal et al., 1996).

To quantify the information given by the empirical counts of dinocyst, sea surface temperatures (SSTs) for February and August were calculated according to the statistical procedure developed by Guiot (1990) and subsequently applied to dinocyst assemblages by de Vernal et al. (1993, 1997, 2001). The database used for the calculation includes 677 surface sediment samples (http://www.geotop.uqam.ca/; http://www.pangaea.de). The SST-calculation procedure is adapted from the Guiot and Goeury (1996) 3P-Base software, and is extensively described in de Vernal et al. (2001). Validation exercises have demonstrated an accuracy (prediction error) of ± 1.3°C and ± 1.8°C in calculating the SSTs for February and August, respectively.

To know where the Holocene samples fit with the MIS 5 sample set, a multivariate analysis (Principal Component Analysis or PCA) was performed on the dinocyst relative abundance data using the software of Guiot and Goeury (1996). 19 taxa and taxon-associations were tested for the 111 samples (i.e. Table 2). The taxon associations result from the groupings made for the SST reconstructions (see de Vernal et al., 2001, p. 684).

4. Dinocyst results

More than 33 dinocyst taxa (Appendix 1; data available upon request) were recognised in each of the studied sections from core MD95-2015 (Eynaud, 1999). In the section corresponding to MIS 5, *Operculodinium centrocarpum*, *Bitectatodinium tepikiense* and *Nematosphaeropsis labyrinthus* alternatively dominate the dinocyst assemblages (Fig. 3). *Spiniferites mirabilis* makes up 20–40% of the assemblages in the lower part of the record, essentially during MIS 5e and 5d. *Brigantedinium* spp., cysts of *Pentapharsodinium dalei* and *Spiniferites elongatus* also are subordinate species in some time intervals. The average dinocyst concentrations are nearly 5000 cysts/cm^3, with major peaks in the middle of MIS 5e where concentrations up to 28 500 cysts/cm^3 are recorded.

In the Holocene section of core MD95-2015 (Fig. 3), dinocyst assemblages are dominated by *Operculodinium centrocarpum*, *Nematosphaeropsis labyrinthus*, cysts of *Pentapharsodinium dalei* and *Brigantedinium* spp. The species *Spiniferites mirabilis* and *Spiniferites elongatus* are subordinate, whereas *Bitectatodinium tepikiense* reaches only up to 5%. The average cyst concentration of 14 500 cysts/cm^3 is high for this part of the record

Table 2
Result of the multivariate analysis (PCA) performed on the dinocyst data of core MD95-2015

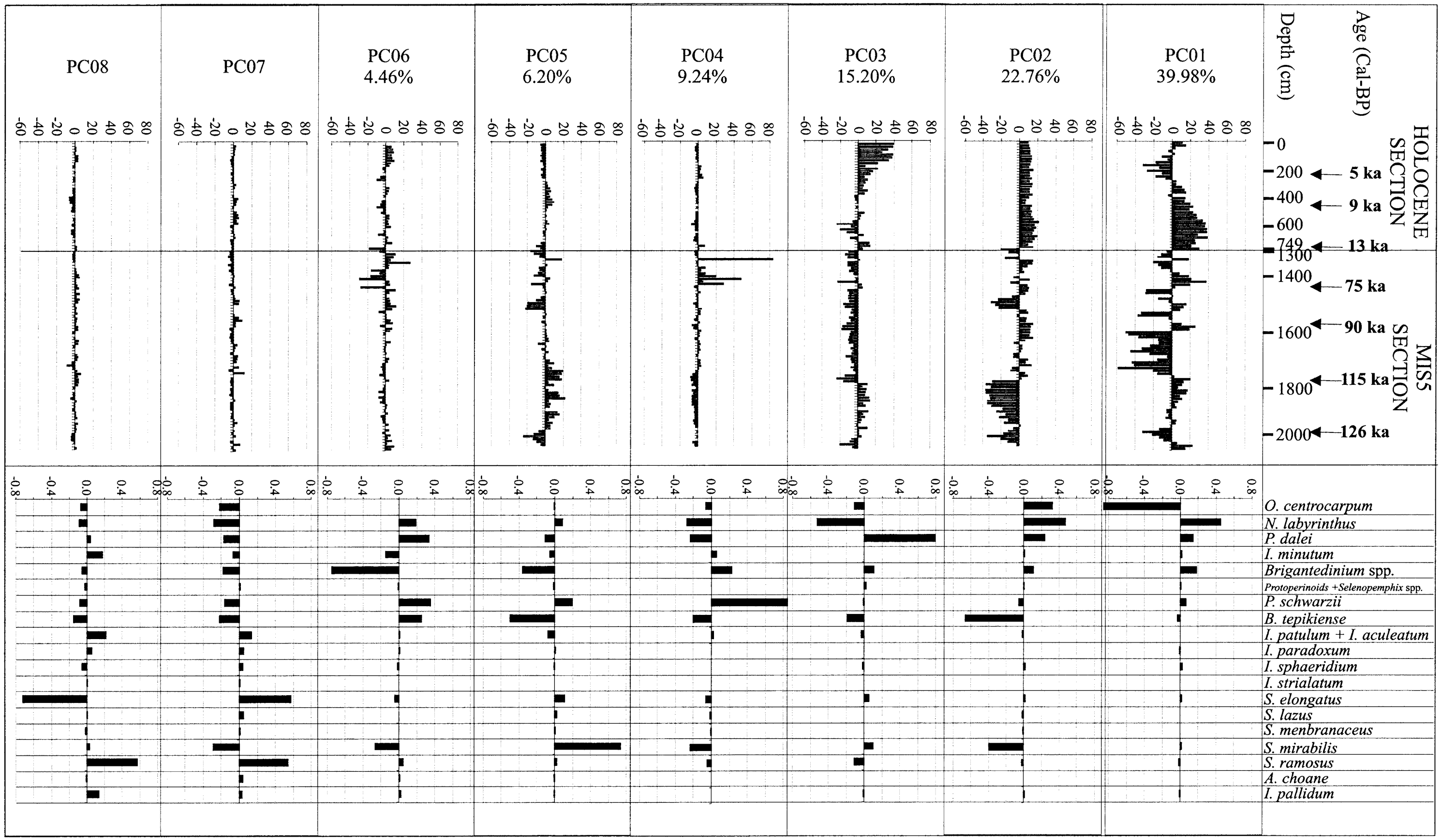

The five first components explain 93.38% of the total variance.

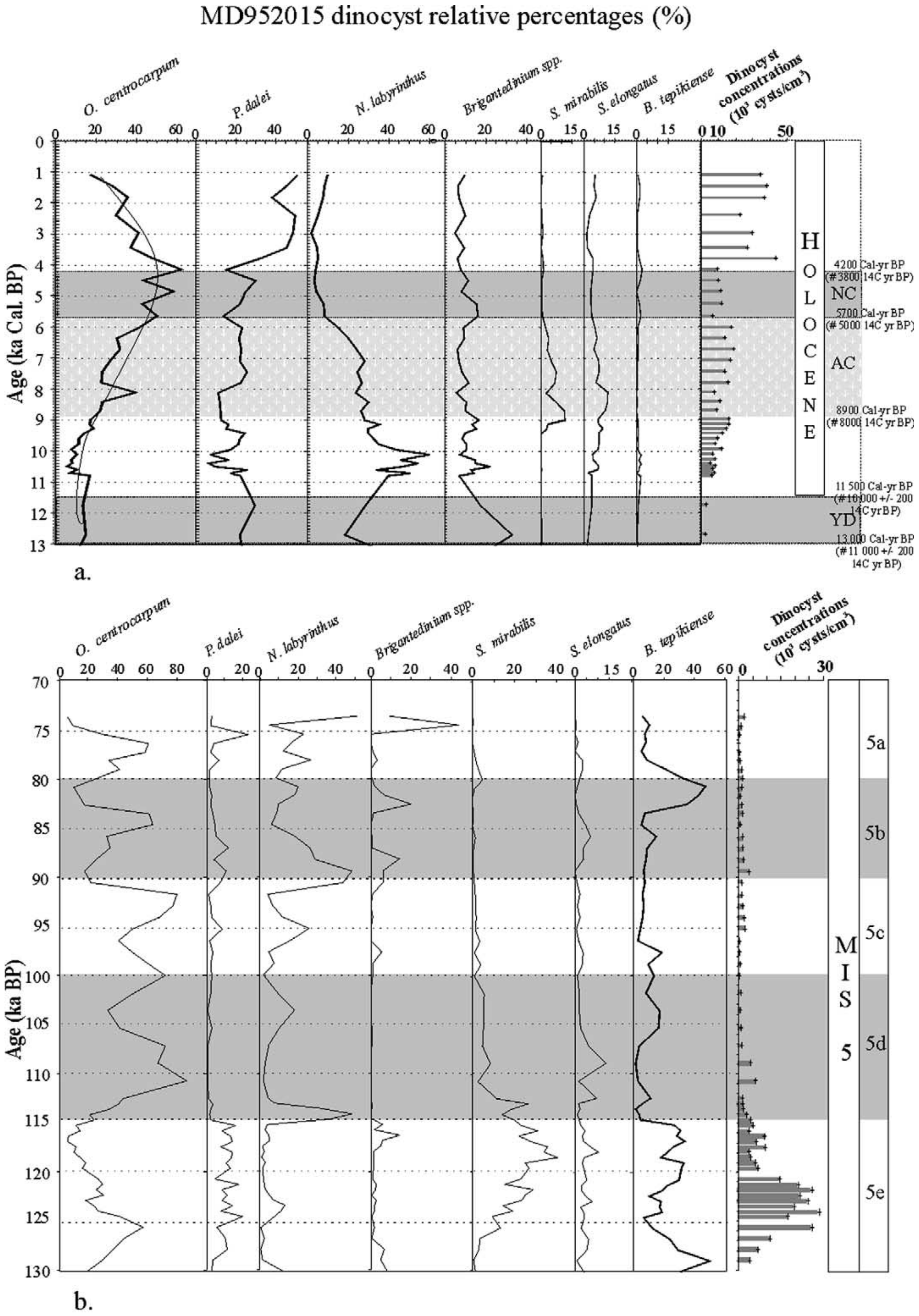
MD952015 dinocyst relative percentages (%)
O. centrocarpum
P. dalei
N. labyrinthus
Brigantedinium spp.
S. mirabilis
S. elongatus
B. tepikiense
Dinocyst concentrations (10³ cysts/cm³)
Age (ka Cal. BP)
HOLOCENE
NC
AC
YD
4200 Cal-yr BP (#3800 14C yr BP)
5700 Cal-yr BP (#5000 14C yr BP)
8900 Cal-yr BP (#8000 14C yr BP)
11 500 Cal-yr BP (#10 000 +/- 200 14C yr BP)
13 000 Cal-yr BP (#11 000 +/- 200 14C yr BP)
a.
Age (ka BP)
MIS 5
5a
5b
5c
5d
5e
b.

with a maximum concentration of up to 44 000 cysts/cm^3 in the upper part of the Holocene.

The multivariate analyses (PCA) have produced eight axes, with the first five axes (PC01, PC02, PC03, PC04, PC05) explaining 93.38% of the total variance. Results of the PCA show a grouping of the analysed samples in relation to coherent climato–stratigraphical units (see Table 2). PC01 has its maximum representation at the base of the Holocene and in some isolated events of the MIS 5, including the late part of the MIS 5e. PC01 is characterised by high positive values for the species *Nematosphaeropsis labyrinthus* and *Brigantedinum* spp. and high negative values for *Operculodinium centrocarpum*. PC02 shows an homogeneous representation throughout the complete Holocene section and is negatively correlated to the Eemian section (sensu stricto: Kukla et al., 2002). The species that display positive PC02 values are *O. centrocarpum*, *N. labyrinthus* and cysts of *Pentapharsodinium. dalei*. PC02 is also characterised by negative values for *Bitectatodinium tepikiense* and *Spiniferites mirabilis*. PC03 marks the samples of the late Holocene and the Eemian section. PC03 shows high positive values for cysts of *P. dalei*, and high negative values for *N. labyrinthus*. PC04 (9.24%) marks samples from the beginning of MIS 4 which will not be discussed here. Cysts of *Polykrikos schwarzii* have high positive PC04 values. PC05 (6.2%) clearly identifies MIS 5e and displays high positive values for *S. mirabilis*.

5. Discussion

5.1. Ecological significance of the dominant dinocyst taxa

Operculodinium centrocarpum, *Bitectatodinium tepikiense*, *Nematosphaeropsis labyrinthus*, *Brigantedinium* spp. and cysts of *Pentapharsodinium dalei* are currently present in surface sediments from the subpolar basins of the North Atlantic Ocean (Rochon et al., 1999).

Since the first biogeographic studies of dinocyst assemblages in recent sediments (Williams, 1971; Wall et al., 1977; Turon, 1981; Harland, 1983), *Operculodinium centrocarpum* has always been considered as a cosmopolitan and temperate taxon. In the surface sediments from the North Atlantic, this species is preferentially distributed along the path of the NAD and is thus assumed to thrive in these warm, saline waters (Turon, 1981, 1984; Harland, 1983; Dale, 1996; Rochon et al., 1999). Nevertheless, this species also occurs in Arctic environments, where endemic morphotypes have been observed (de Vernal et al., 2001). The present study (Fig. 3) shows that the distribution of *O. centrocarpum* is not constrained to the interglacial periods, as some peaks in abundance also occur during cold phases of the interglacial sections. The palaeoceanographic and climatic implications of this signal are discussed in further detail in Section 5.2.2.

Bitectatodinium tepikiense is at present mainly distributed from temperate to sub-Arctic environments of the North Atlantic, with maximum representation south of the Gulf of St. Lawrence (Rochon et al., 1999; de Vernal et al., 2001). This species tolerates large seasonal variations in temperature, with very cold winters (as cold as 1°C) and mean summer temperatures over 15°C. It also thrives in a wide range of salinities (30–35). *B. tepikiense* has been observed in Quaternary sediments off the Portugal margin (Eynaud et al., 2000; Boessenkool et al., 2001; Turon et al., in press), where it has been linked to the southward penetration of cold subpolar waters during Heinrich or Heinrich-like events. Dinocyst studies on the cold MIS 4 and 6 of cores MD95-2015 and MD95-2014 have similarly revealed very high percentages of *B. tepikiense* (up to 80% of the dinocyst assemblages during MIS 6; Eynaud, 1999). In

Fig. 3. Dominant dinocyst species distribution (relative percentages) along the studied sections of core MD95-2015. (a) Limits in age of the Younger Dryas (YD) cold event conforming to those cited in Bard (1998). The Neoglacial Cooling (NC) period is defined by Koç et al. (1996) and the Atlantic Chronozone (AC) as delimited by Jansen and Bjørklund (1985). (b) Limits of the 5e/5d transition positioned according to Shackleton et al. (2002).

the MD95-2015 interglacial records, *B. tepikiense* comprises up to 60% of the total dinocyst assemblage. These high abundances could mark the influence of strong and cold fronts nearby, maybe linked to the latitudinal displacements of the IC throughout time. Nevertheless, such high abundances are only recorded at the base of the last interglacial complex (MIS 5), during the probable 'Younger Dryas-like event' of Termination II (Sarnthein and Tiedemann, 1990; Seidenkrantz, 1993; Maslin et al., 1998; Sanchez-Goñi et al., 1999; Eynaud et al., 2000). The *B. tepikiense* cysts have by contrast to the base of MIS 5, very limited relative abundances during the Holocene period. During MIS 5, the occurrence of *B. tepikiense* seems also to be linked to transition periods between cold and warm substages and vice versa. High percentages are indeed present at the transition between MIS 5b and MIS 5a (Fig. 3). The association of *B. tepikiense* with *Spiniferites mirabilis* and *Operculodinium centrocarpum* in interglacial substages is surprising considering their ecological respective affinities. It has, nevertheless, already been reported from two ODP sites (LEG 105, Sites 646 and 647) in the Labrador Sea by Aksu et al. (1989). Results of the PCA also confirm this association: *B. tepikiense* and *S. mirabilis* are negatively correlated to PC02, and shed light on a non-analogous situation between the Eemian and the Holocene (Table 2).

Nematosphaeropsis labyrinthus is a typical oceanic species, which is mainly distributed between 45 and 65°N in the North Atlantic Ocean (Rochon et al., 1999). In the Alborean Sea, Turon and Londeix (1988) have shown that this taxon is associated with nutrient-rich cool waters. Recent work based on the modern analogue approach also demonstrate this characteristic for the Atlantic Ocean (Devillers and de Vernal, 2000). In the Portuguese margin sediments, *N. labyrinthus* was found in close association with *Bitectatodinium tepikiense*, characterising cold polar water episodic intrusions (Eynaud et al., 2000). In the MD95-2015 record, *N. labyrinthus* has an average abundance of 13% during MIS 5. Consistently, peaks are recorded at the beginning of cold substages (5d and 5b). Similar peaks were also observed from MIS 5 at the Barents Sea margin but were not precisely constrained with the stratigraphy (Matthiessen and Knies, 2001). During the Holocene, *N. labyrinthus* represents 24% of the dinocyst assemblages (average value on the whole section). Its maximum occurrence (up to 60%) is recorded early in the Holocene between 11.5 and 9.5 cal kyr BP (10–8.5 ^{14}C-kyr BP). It is worth noting that throughout the MD95-2015 record, *N. labyrinthus* appears to be linked to transitional climatic periods. Compilation of *N. labyrinthus* records in the North Atlantic ocean for the last 150 000 years suggest optimal occurrence of this species during short events of severe hydrological changes (Turon and Eynaud, unpublished data).

Brigantedinium spp. tolerates seasonal sea-ice cover but, as a heterotrophic taxon, its occurrence is also linked to food availability (especially small prey such as diatoms). In the MD95-2015 interglacial records, *Brigantedinium* spp. are not well represented and only appear during discrete events (also confirmed by PCA). Notably, *Brigantedinium* spp. are the dominant species of the Younger Dryas interval. Some taphonomic effects concerning the preservation of this cyst in the sediment could be considered, as it has been shown that it is very sensitive to oxygenated conditions (Zonneveld et al., 1997, 2001). The location of the core, just under the influence of the highly oxygenated water of the North Atlantic Deep Waters would favour such taphonomic modification of the dinocyst signal. Nevertheless, the comparison of *Brigantedinium* spp. percentages vs. the dinocyst total concentration do not support such a bias, as no co-variation could be observed. In fact, if taphonomic artefacts have modified the *Brigantedinium* spp. record, it is logical to consider that the whole dinocyst community would have been affected by the same processes.

Cysts of *Pentapharsodinium dalei* occur today in sediments from polar to subpolar environments that experience summer temperatures higher than 4°C (Rochon et al., 1999). It has also been reported from sediments from the Gulf of Guinea (Marret and Turon, 1994). In core MD95-2015, cysts of *P. dalei* preferentially occur during MIS 5e and in the late Holocene (Fig. 3). Results of the PCA also confirm this observation (Table 2): from the PCA we could therefore deduce that cysts of *P. dalei* are the only species in the South Icelandic Basin supporting an analogy between the Eemian and Holocene periods.

The other significant species recorded in the studied sections is *Spiniferites mirabilis*. This species is known to mark warm temperate to temperate environments (Turon, 1981; Harland, 1983; Turon, 1984; Marret and Turon, 1994; Rochon et al., 1999). Morzadec-Kerfourn (1992) has demonstrated its tropical extension as far south as 10°N. *S. mirabilis* is at present sparsely distributed in the sediments of the North Atlantic Ocean (see Fig. 4a), with a maximum occurrence in the Bay of Biscay (Harland, 1983) and off the coast of Portugal (Rochon et al., 1999). Recent investigations in the occidental Mediterranean Sea surface sediments (Mangin, 2002) have shown that *S. mirabilis* is a major component of the Mediterranean dinocyst assemblages (more than 20%), therefore confirming its thermophilic character. Correlation of the hydrological parameters of the $n = 677$ data base (de Vernal et al., 2001) to the percentage abundance of each taxon could better constrain the ecology of modern dinocysts. It has been demonstrated that for *S. mirabilis* its highest percentage abundance occurs at winter SSTs between 10 and 15°C and at summer SSTs between 15 and 22°C; these are assumed to reflect the optimum thriving conditions of *S. mirabilis*.

5.2. *The* Spiniferites mirabilis *and* Operculodinium centrocarpum *records from MIS 5 and the Holocene*

The following discussion concentrates on the two temperate species recorded in the MD95-2015 interglacial records: *Spiniferites mirabilis* and *Operculodinium centrocarpum*. The relative abundances and concentrations of these species are used as a semi-quantitative tool to monitor maximum SST in the South Icelandic Basin. We note here the quasi-absence of the warm cysts *Impagidinium aculeatum* and *I. patulum*, which, in association with *S. mirabilis*, are used classically (Turon and Londeix, 1988; Boessenkool et al., 2001; Versteegh, 1994; Turon et al., in press) to identify episodes of climatic optima in southern latitudes (Portugal Margin, Alboran Sea).

5.2.1. Spiniferites mirabilis *record*

Higher percentages of *Spiniferites mirabilis* clearly mark the MIS 5e and MIS 5d substages (Fig. 3). The percentages (up to 40%) recovered in the MIS 5e interval of core MD95-2015, therefore at a location (59°N) close to its present northernmost limit of occurrence, indicates a significant latitudinal displacement of its biogeographical distribution centre and suggests that MIS 5e experienced warmer conditions than today. This result confirms the previous finding of Matthiessen and Knies (2001) and in general for the last interglacial periods (Kukla et al., 2002). Substage 5d shows, surprisingly, the persistence of *S. mirabilis* until the transition towards Substage 5c. It means that the cool period of Substage 5d has not been so drastically marked in the dinocyst assemblages of the South Icelandic Basin. It conforms to the recent re-evaluation of the Eemian duration on the basis of marine pollen sequences analysis (Sánchez-Goñi et al., 2000; Shackleton et al., 2002) and to recent works in the North Atlantic (McManus et al., 2002). The interglacial/glacial shift towards cooler conditions is however depicted in the dinocyst concentrations, as the maximum abundances are strictly constrained to the thermal optimum of MIS 5e.

In the Holocene section the occurrence of *Spiniferites mirabilis* fits well (Fig. 3) with the Atlantic Chronozone (AC) as time-delimited in marine records by Jansen and Bjørklund (1985) between 8900 and 5700 cal yr BP (8000–5000 ^{14}C yr BP). Summer temperatures during this interval were higher in Northern Europe than present-day temperatures. The Atlantic Chronozone was therefore interpreted as the Holocene hypsithermal and used by modellers as a future scenario in the context of a global warming (e.g. Gajewski et al., 2000). The cooling tendency observed in the more recent part of the core is in agreement with the modern biogeographical distribution of *S. mirabilis* (1% at the core latitude; Fig. 4a).

By 8.2 cal kyr BP (380 cm depth in the core), we observe a clear decrease in both *Spiniferites mirabilis* percentages and concentrations. There

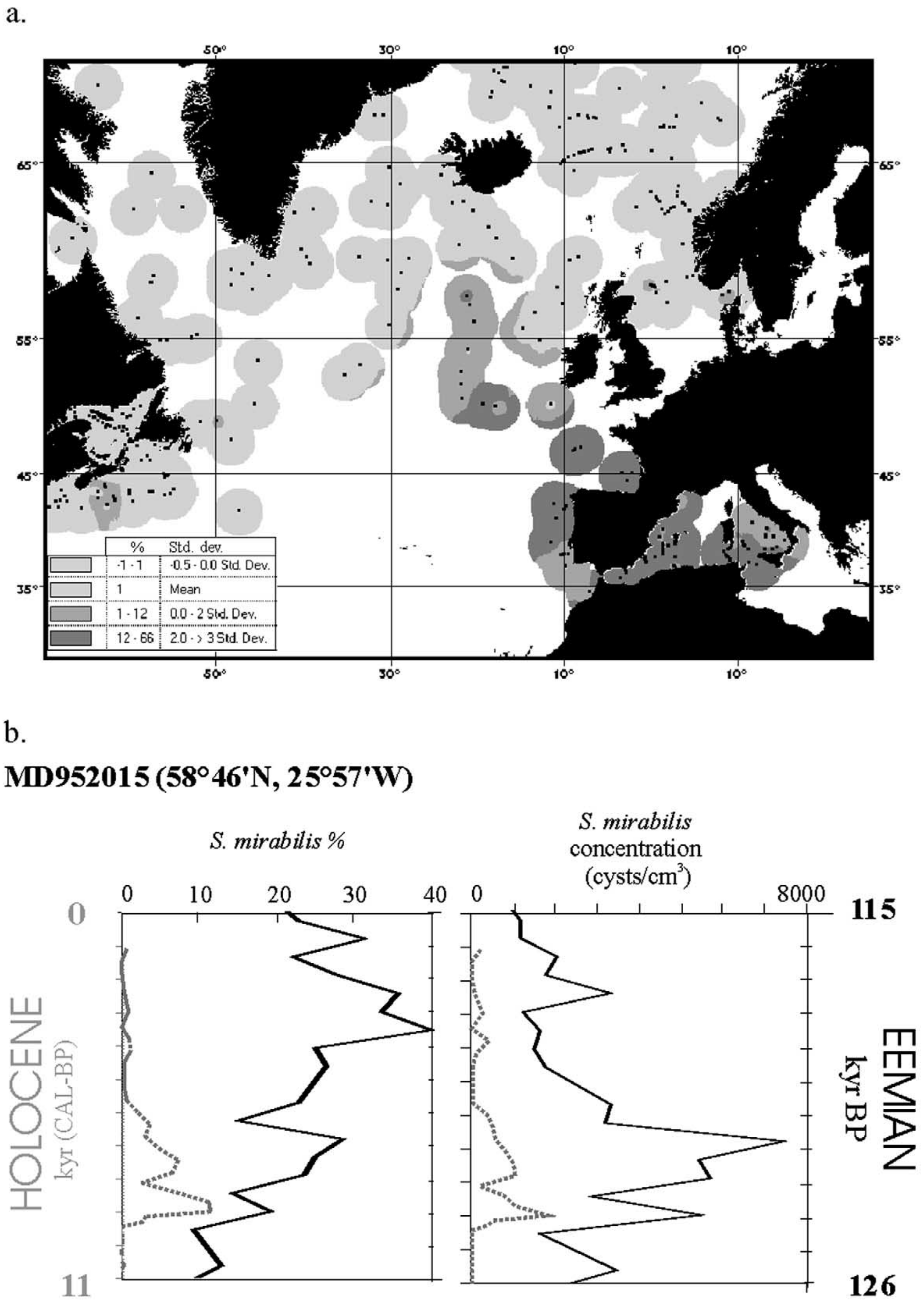
a.
50°
30°
10°
10°
65°
55°
45°
35°
% | Std. dev.
-1 - 1 | -0.5 - 0.0 Std. Dev.
1 | Mean
1 - 12 | 0.0 - 2 Std. Dev.
12 - 66 | 2.0 - > 3 Std. Dev.
b.
MD952015 (58°46'N, 25°57'W)
S. mirabilis %
0
10
20
30
40
S. mirabilis concentration (cysts/cm^3)
0
8000
0
11
HOLOCENE
kyr (CAL-BP)
115
126
EEMIAN
kyr BP

is no doubt that this decrease corresponds to the '8.2 cooling event' initially observed in the $\delta^{18}O$ signal of Greenland Ice records (Alley et al., 1997; Leuenberger et al., 1999) and since largely documented in the Northern Hemisphere (e.g. Klitgaard-Kristensen et al., 1998; von Grafenstein et al., 1998; Nesje and Dahl, 2001; Yu and Wright, 2001; Baldini et al., 2002; Dean et al., 2002). Genetic mechanisms of this distinctive climatic shift have been linked to a catastrophic meltwater input from the waning Laurentide Ice-Sheet in the Labrador Sea (draining of the Agassiz and Ojibway lakes; Barber et al., 1999).

Fig. 4b presents the comparison of the percentages and concentrations of *Spiniferites mirabilis* in core MD95-2015 plotted along the last 11 cal kyr BP and the first 11 kyr of the Eemian (as defined by Shackleton et al., 2002; Kukla et al., 2002), a more recent analogue for the Holocene. Fig. 4b shows that the highest percentages of *S. mirabilis*, up to 40%, are reached in the second part of MIS 5e (117–118 kyr BP), whereas the highest concentrations are only restricted to the middle of MIS 5e, around 122 kyr BP. This scheme is linked to the dinocyst total concentrations that peak precisely at 122 kyr BP. When comparing the Holocene and Eemian sections (Fig. 4b on the right), the concentration profiles of *S. mirabilis* are very similar. This observation is difficult to apply to the relative percentages (Fig. 4b on the left). The good coherence of the *S. mirabilis* concentration evolution throughout the Holocene and the Eemian, with especially a marked peak of abundance in the first part of these two periods could be due here to a sedimentary or taphonomic artefact. In fact, these peaks at the deglaciation onset, could traduce enhanced deep circulation as a result of the re-initiation of the deep-convection in the Nordic Seas. Nevertheless, no coherence observed in the whole dinocyst concentrations justifies this interpretation. The combined information brought by *S. mirabilis* percentages and concentrations, however, allows us to conclude that only two maxima of *S. mirabilis* occurrence have been recorded during the last 130 000 years in the South Icelandic Basin. These maxima are respectively located between 126 and 120 kyr BP, and from 9.2 to 5.7 cal kyr BP (~8–5 ^{14}C kyr BP).

5.2.2. *Operculodinium centrocarpum* record

Operculodinium centrocarpum is a cosmopolitan species widely distributed in the surface sediments of the North Atlantic Ocean. In the modern dinocyst data base $n = 677$ (de Vernal et al., 2001), this species occurs as a dominant taxon in a wide range of environments (Fig. 5a), therefore showing no real optimum distribution with regard to SST. In the MD95-2015 interglacial records, percentages of *O. centrocarpum* are high, with an average value of 35% for MIS 5 and 25% for the Holocene section (see Fig. 3). These high percentages are in agreement with its present distribution pattern in surface sediments of the North Atlantic Ocean, which appears to be closely linked to the surface circulation pattern of the NAD (Rochon et al., 1999). Surface sediments underlying the IC, which is a return branch of the NAD, display *O. centrocarpum* percentages exceeding 40%.

The 50-kyr duration of the MIS 5 *Operculodinium centrocarpum* record depict a gentle oscillating scheme (Fig. 5b). After the termination of Substage 5e, the recurrence of marked peaks of relative abundances (over 60%) are recorded every 7–8 kyr. These peaks occur during warm/interstadial substages as well as during cold/stadial substages. They are correlated with maxima in

Fig. 4. (a) Present day distribution of *Spiniferites mirabilis* cysts in recent sediments of the North Atlantic Ocean and the Mediterranean Sea. The modern 'Dinocyst $n = 677$' data base (de Vernal et al., 2001) plus 90 Mediterranean points (Mangin, 2002) were used to map the distribution of *S. mirabilis* using Arcview GIS. The previous finding of Harland (1983) is confirmed, i.e. the centre of distribution for this species in the north Atlantic is located in the Bay of Biscay; the extensive distribution of this taxon in the Mediterranean Sea is also highlighted. (b) Comparison of fluctuations in *Spiniferites mirabilis* abundance throughout the Holocene and the first 11 kyr of the Eemian section (Eemian age limit definition after Shackleton et al. (2002) and Kukla et al. (2002)). Holocene data are shown in grey (dotted line) and Eemian data in black.

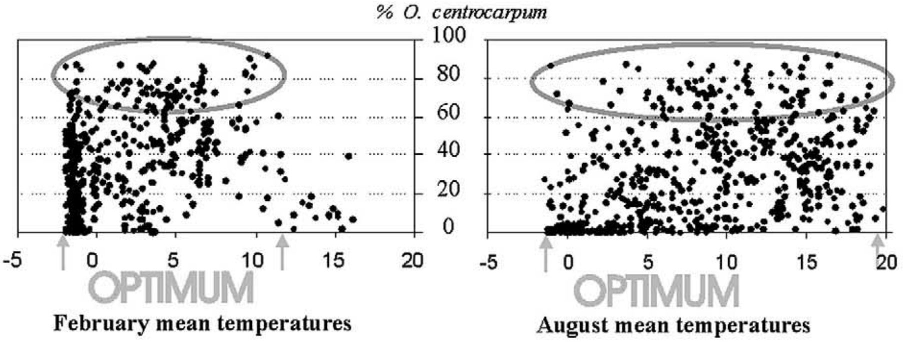
% O. centrocarpum
100
80
60
40
20
0
-5
0
5
10
15
20
OPTIMUM
February mean temperatures
OPTIMUM
August mean temperatures

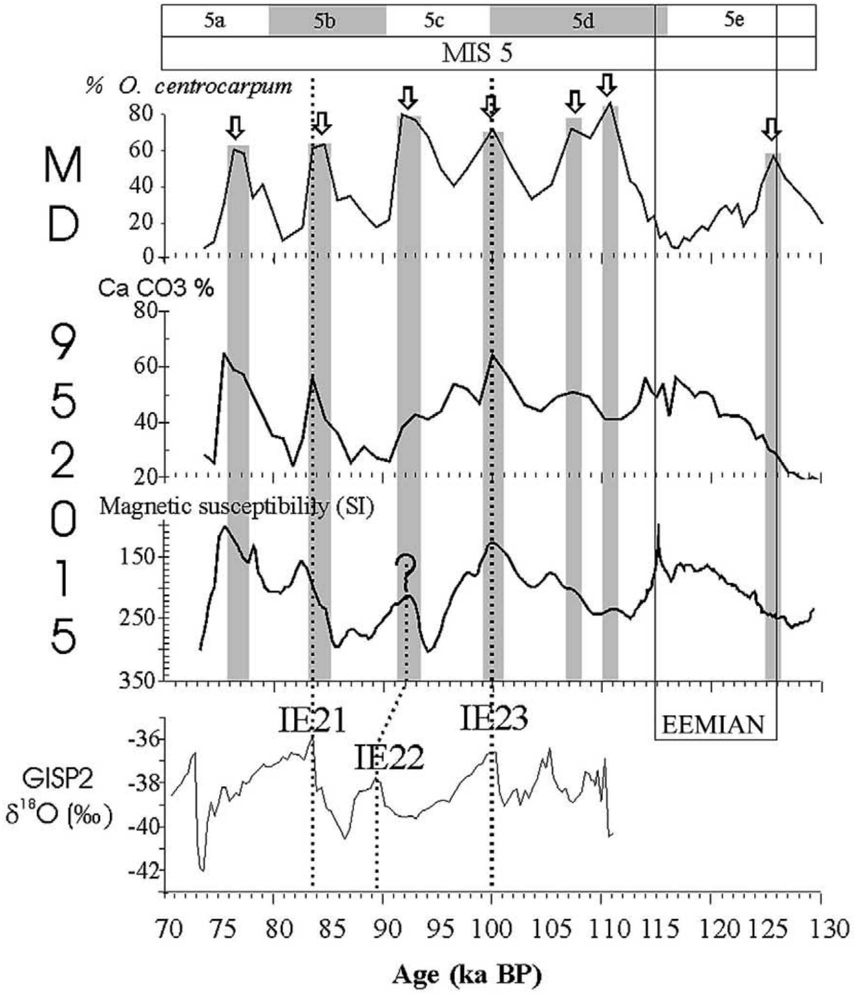
5a
5b
5c
5d
5e
MIS 5
% O. centrocarpum
M
D
9
5
2
0
1
5
80
60
40
20
0
Ca CO3 %
80
60
40
20
Magnetic susceptibility (SI)
150
250
350
?
IE21
IE22
IE23
EEMIAN
GISP2
δ18O (‰)
-36
-38
-40
-42
70
75
80
85
90
95
100
105
110
115
120
125
130
Age (ka BP)

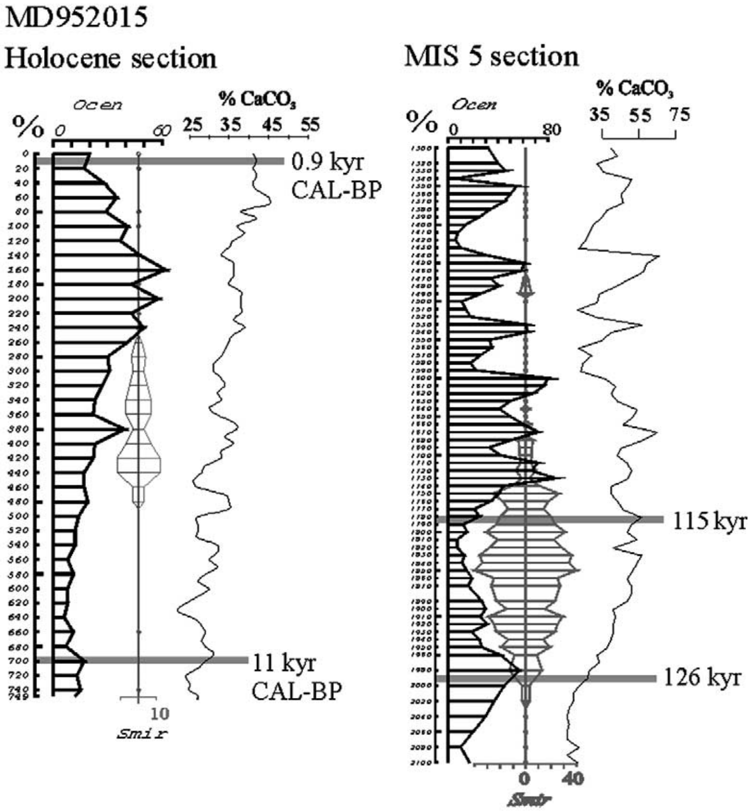

Fig. 6. Comparison with depth of the warm dinocyst species (*Operculodinium centrocarpum* and *Spiniferites mirabilis*) percentages with $CaCO_3$ contents (%).

$CaCO_3$ contents (Fig. 6) and with low values of magnetic susceptibility (MS). Maximum $CaCO_3$ contents are classically assumed to reflect warm conditions linked to events of high carbonate productivity or/and accumulation. In core MD95-2015, the synchronous low values of MS support this assumption, actually reflecting dilution of the terrigeneous signal by diamagnetic material (carbonate, biogenic opal…). As explained above (Section 3.1), some of these events were used as tie-points with the GISP ice-core stratigraphy to construct a stratigraphic framework for core MD95-2015 (Interstadial Events IE21 and IE23).

The Holocene section and the MIS 5 section (Fig. 6) depict a coherent pattern for the dinocyst and the carbonate proxies, that globally record the same changes through time. These support and reinforce the link between high carbonate content and warm conditions as evidenced by the dinocyst assemblages.

The coherence of the $CaCO_3$, MS and *Operculodinium centrocarpum* signals downcore argues

Fig. 5. Comparison of the *Operculodinium centrocarpum* percentages with the magnetic susceptibility and $CaCO_3$ content data along the MIS 5 section of core MD95-2015. GISP2 $\delta^{18}O$ data are plotted on the same age scale for discussion. Arrows and grey bars mark the *O. centrocarpum* percentage peaks. The Eemian period is plotted according to Shackleton et al. (2002). The top of the figure presents the distribution of *O. centrocarpum* percentages vs. SST (February and August) in the modern data base (de Vernal et al., 2001).

for a common process driving the depositional mechanism of these three proxies. The Gardar Drift is a giant contourite drift. Contourites are known to be constructed by deep-sea geostrophic flows that occur preferentially during sea-level high stands, i.e. interglacial periods (Faugères et al., 1993, 1999). This is verified in the case of our study, as core MD95-2015 records higher sedimentation rates during interglacial stages (Giraudeau et al., 2000). In the Northern Hemisphere, contourite drifts are constructed on the right of the main bottom current axis (NADW for the Gardar Drift). All the material that settles from overlying water masses is accumulated in this way, as is the fine material transported by the current itself. High *O. centrocarpum* percentages coherent with high $CaCO_3$ contents argue for warm climatic shifts. That would mean, in agreement with the thermohaline circulation model of Broecker et al. (1990) that the NAD northward penetration, as well as the NADW formation, would be enhanced during these combined *O. centrocarpum* and $CaCO_3$ peaks. That is at least what should be expected considering that *O. centrocarpum* has always been considered as a tracer of the NAD penetration (Turon, 1981, 1984; Harland, 1983; Dale, 1996; Rochon et al., 1999).

The Holocene record (Fig. 3) of *Operculodinium centrocarpum* displays a maximum occurrence of this species during the Neoglacial cooling phase (as defined in Koç et al., 1996). This result could be in conflict with the thermophilic character of *O. centrocarpum*. Nevertheless, considering the location of core MD95-2015 under the influence of the IC, a possible explanation of this result could be found in the balance between the intensity of the NAD penetration into the Norwegian Sea and the intensity of its return branch stream, i.e. the IC (Orvik et al., 2001). Preferential flow of the IC, in response to the weakening of the NAD during the Neoglacial cooling, should have generated high occurrences of *O. centrocarpum* in core MD95-2015 since this core lies directly under the influence of the IC. Eiríksson et al. (2000) have shown a period of high influence of the IC to the northern Icelandic shelf between 4600 and 3000 cal yr BP.

In the Southern Icelandic Basin, *Operculodinium centrocarpum* (percentage abundance) may therefore be used to monitor variations in intensity of the NAD circulation and recirculation. Two modes can be distinguished: (1) enhanced NAD with an efficient transport towards polar basins, and (2) weakened NAD but enhanced IC. The last mode would have occurred during relatively cold phases of interglacial complexes.

5.3. Dinocyst data vs. planktonic foraminiferal data

A comparison of the dinocyst vs. the planktonic foraminiferal data for the last 13 000 years is presented in Fig. 7; independent SST reconstructions for the two proxies are included. For discussion, only selected dinocyst and foraminiferal species are presented on the graph (*Operculodinium centrocarpum*, *Spiniferites mirabilis*, *Nematosphaeropsis labyrinthus*, and *Globorotalia inflata*). SST reconstructions from the foraminiferal datasets were calculated according to the Modern Analog Technique (MAT; detailed procedure in Manthé, 1998 – 32 foraminiferal species used for a modern data base of 556 points).

Dinocyst and foraminiferal SST reconstructions

Table 3
Comparison of dinocyst and foraminifer based SST for the last 13 000 cal kyr

Present day	Mean February SST 6.5°C			Mean August SST 11°C		
Last 13 cal kyr	Minimum	Time averaged	Maximum	Minimum	Time averaged	Maximum
Foraminiferal based	5°C	8.8°C	10.4°C	11.3°C	12.7°C	14.3°C
Dinocyst based	−1.5°C	1.5°C	5.5°C	8.1°C	13.8°C	17°C

Modern hydrographic conditions prevailing in surface waters (SST – 0 m depth) overlaying core MD95-2015 were extracted from data published by the National Ocean Data Center (NODC, 1994).

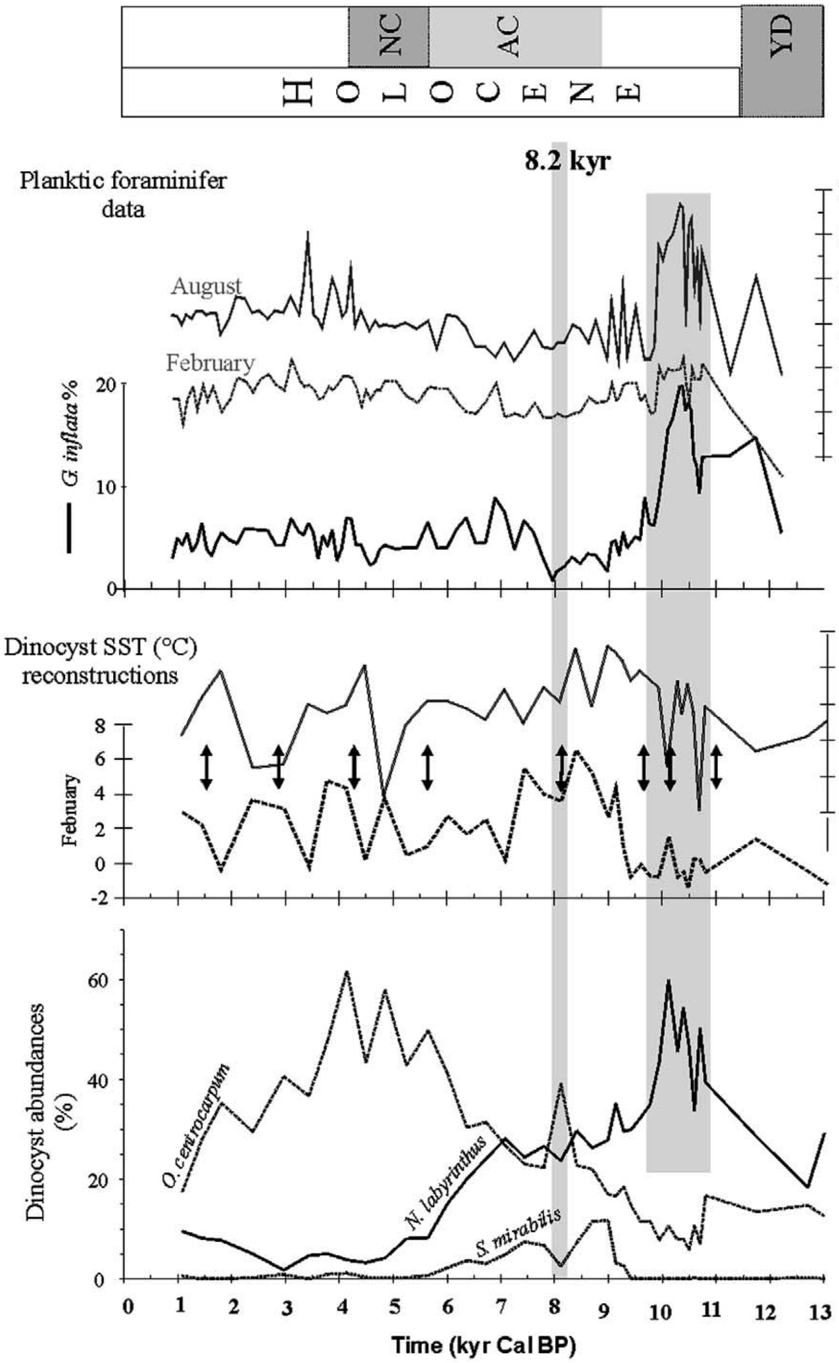

Fig. 7. Comparison of some selected dinocyst and foraminiferal species with the Holocene SST reconstruction (based on dinocysts and foraminifera).

show large discrepancies for the studied interval (Table 3). Compared to present-day SSTs, the two methods overestimate August SST. The February SSTs are also overestimated by the foraminiferal proxy but are clearly underestimated by the dinocyst proxy. These discrepancies could be due to a lack of reference sites under 5°C in winter in the foraminiferal database, and to a lack of reference sites over 5°C in winter for the dinocyst database.

Apart from these discrepancies, large differences are recorded between the SST records. The more prominent feature is that SST maxima do not occur synchronously (Fig. 7): the Holocene optimum as reconstructed by foraminifera is located at the base of the Holocene section (11–9.5 cal kyr BP) whereas it occurs in the middle Holocene (9.5–7 cal kyr BP) according to dinocyst data. The dinocyst results are in good agreement with coccolithophorid assemblages that record warm conditions between 10 and 6 cal kyr, with an optimum centred around 6.5 cal kyr BP (Giraudeau et al., 2000). They also agree with the warm Atlantic Chronozone of Jansen and Bjørklund (1985). Both records (coccolithophorid as dinocyst based), however, show a cooling trend after 6 cal kyr BP, confirming the result of the multiproxy study of Marchal et al. (2002).

The relatively good correlation observed along the record between percentages of the dinocyst *Nematopshaeropsis labyrinthus* and those of the foraminifer *Globorotalia inflata* (Fig. 7) supports the conclusion that the depicted discrepancies in the quantitative estimations of the SST express the ecological particularities of the proxies. An unusual event, occurring between 11 and 9.5 cal kyr BP and where maximum percentages of these two species are observed, especially illustrates this observation. According to planktic foraminiferal reconstructions, this event marks a sea-surface warming. Nevertheless, considering the ecological preferences of *N. labyrinthus*, this event should be reinterpreted in terms of nutrient availability, as this species is actually associated with nutrient-rich waters (Turon and Londeix, 1988; Devillers and de Vernal, 2000). *G. inflata* distribution in the modern foraminiferal database also supports this interpretation. In fact, this species displays high percentages off the coast of Morocco, in a sector directly influenced by the upwelling cell of the northwestern African margin. In this case, *G. inflata* therefore records the double signature of high temperatures and high nutrient availability. The MAT reconstructions, limited to SST, could not trace this particularity. Our study shows, therefore, that comparison of the tracers is a good way to avoid misinterpretation of the data.

Another divergence in the Holocene SST reconstruction is that foraminiferal-based February SSTs are very smooth after 10 cal kyr BP, whereas the dinocyst-based February SSTs reveal several large oscillations (up to 4°C). No a-priori climatic mechanism could justify these oscillations, and the 1.5-kyr cycles identified by Bond et al. (1997) and then recognised in the *Emiliania huxleyi* percentages of core MD95-2015 (Giraudeau et al., 2000) do not match with the dinocyst cycles. These oscillations are accordingly more questionable as the SST signal depicted is often not coherent throughout the seasons, showing on some events a warming in February and a cooling in August (and vice versa). Although dinocysts constitute a very sensitive tool to determine seasonality (de Vernal and Hillaire-Marcel, 2000), the only factor that could justify such SST divergence, we cannot be totally confident about the quantified SST values. So far, no other data have confirmed the dinocyst transfer function results. The MD95-2015 Holocene record shows that information is lacking to enable unambiguous interpretation.

In summary, with regard to quantification results and procedures, the proposed data comparison for the Holocene does not argue for one quantitative method or another. It underlines, however, the subjectivity of the tracer used and especially shows the danger of blind applications of the transfer functions, since each proxy records more that one type of information. Relative percentages are in some case much easier to interpret for the purposes of palaeoceanographic reconstruction.

6. Conclusions

The study of organic-walled dinoflagellate cysts of the interglacial sections of core MD95-2015 (MIS 5, Holocene) has revealed major and minor changes in the identified assemblages; such biological changes are coherent with stratigraphical and palaeoclimatological changes identified in the South Icelandic Basin from other available proxies.

Two dinocyst species especially have displayed significant results: *Spiniferites mirabilis*, that depicts an apparent blooming phenomenon during the interglacial optima, and *Operculodinium centrocarpum* that seems to monitor the North Atlantic Drift/IC pulsations in the South Icelandic Basin.

Combined data of *Spiniferites mirabilis* concentrations and percentages allow the identification of only two marked periods of occurrence of this taxon, i.e. at the base of MIS 5 and in the middle of MIS 1. This species occurs in significantly larger proportions during the Last Interglacial Period (MIS 5e) than during the Holocene, thus suggesting a warmer climate during the Last Interglacial. Nevertheless, its association with *Bitectatodinium tepikiense* at this period underlines a non-analogous situation between the two interglacial sequences. PCA on the whole dinocyst community also confirms this observation (especially prominent on PC02 – 22.76% of the variance). Our data, however, confirm that *S. mirabilis* alone could represent a useful climato–stratigraphical tool to identify thermal optima in the subpolar basin of the North Atlantic Ocean.

Throughout the studied interglacial sections, *Operculodinium centrocarpum* occurrence is characterised by large peaks in relative abundance that are recorded during warm periods as well as cold periods. These percentage fluctuations seems to reflect variation in the intensity of the deep and sea-surface circulation of the region.

In the Holocene section, dinocyst results were occasionally in conflict with the other proxy of sea-surface parameters that planktic foraminifera represent. We could nevertheless infer, on the basis of our study, that the beginning of the Holocene seems to be marked by an episode of nutrient-rich cool waters in the South Icelandic Basin. This was followed by a period with higher SSTs from 9 to 6 cal kyr BP (8–5.2 ^{14}C kyr BP) that matches with the Atlantic Chronozone.

With regards to the tools used for this study, comparison of the dinocyst based reconstructions with the planktonic foraminiferal ones have shown the limitations of the statistical quantitative approaches. In some cases the ecological information is oversimplified, leading to palaeoclimatic misinterpretations. This highlights the importance of multiproxy approaches, as they offer improved discrimination among various ecological forcing parameters.

Acknowledgements

This work has been funded by the French MENRT and the CNRS. Financial support for the analysis is from EC contract ENV4CT 970643 and the PNEDC. We wish to thank Mr. Y. Balut, the captain, and crew of the RV Marion Dufresne (IPEV) for their assistance at sea, M.H. Castera and O. Ther for preparing the sample. The manuscript has been significantly improved by the reviews of Drs. G. Versteegth and G.J. Wilson. We are grateful to Graham Forsythe for improving the English text. Most of the ^{14}C and δ^{18}O analyses have been performed at the LSCE (Gif-sur-Yvette, France). This is DGO/UMR EPOC 5805 Contribution No. 1470.

Appendix 1

Taxonomic list of the dinoflagellate cyst taxa from this study (Fig. 8). The identification of the dinoflagellate cysts follows Turon (1984) and Rochon et al. (1999). The nomenclature conforms to Williams et al. (1998) et Head et al. (2001).

Division: DINOFLAGELLATA Bütschli, 1885 Fensome et al., 1993
Subdivision: DINOKARYOTA Fensome et al., 1993
Class: DINOPHYCEAE Pascher, 1914
Order: GONYAULACALES Taylor, 1980
Family: GONIODOMACEAE Lindeman, 1928

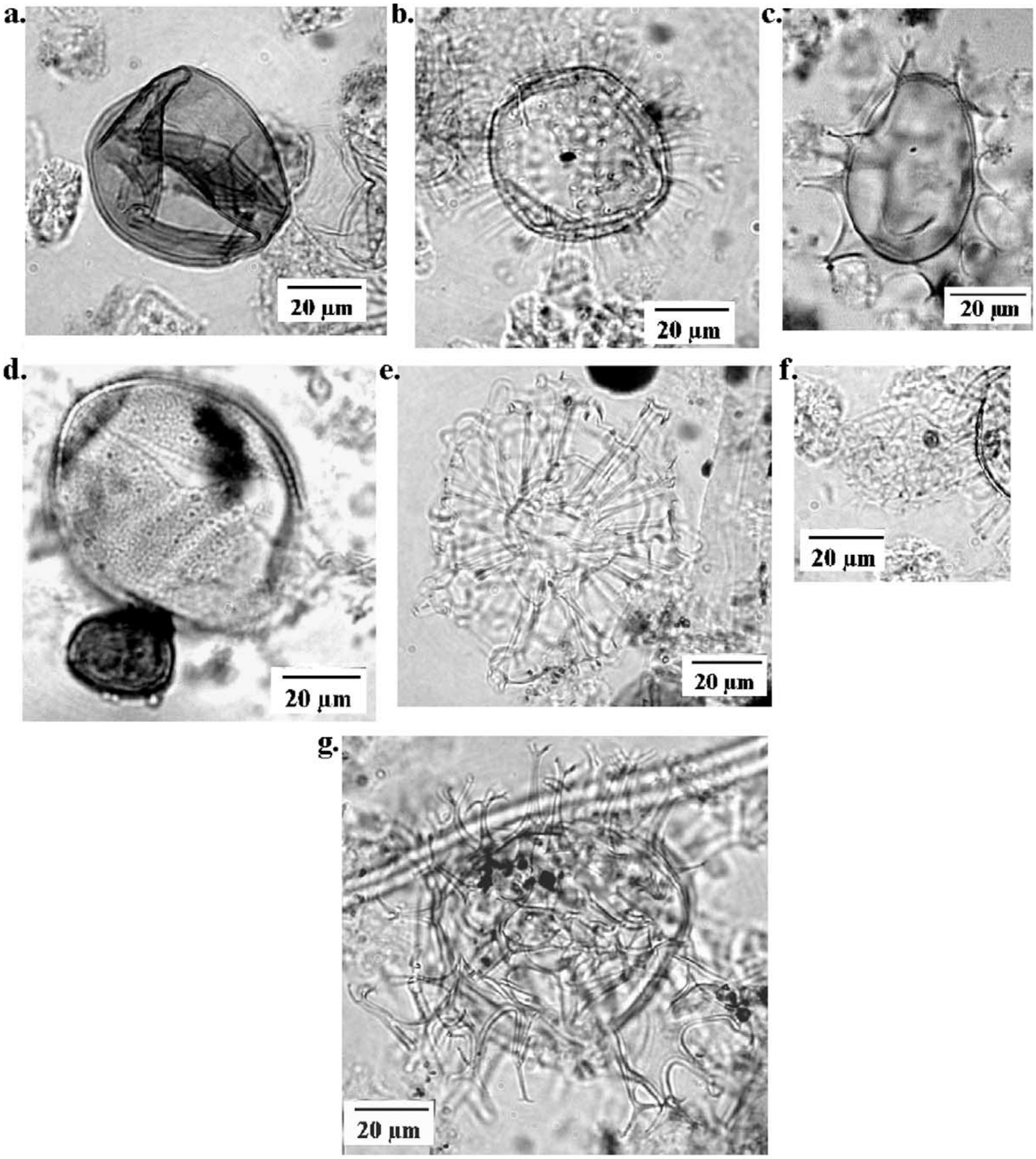

Fig. 8. Photomicrographs of the dominant dinoflagellate cyst taxa from this study (×400). (a) *Brigantedinium* spp., MD95-2015-0 cm. (b) *Operculodinium centrocarpum*, MD95-2015-0 cm. (c) *Spiniferites elongatus*, MD95-2015-0 cm. (d) *Bitectatodinium tepikiense*, MD95-2015-1510 cm. (e) *Nematosphaeropsis labyrinthus*, MD95-2015-1510 cm. (f) *Pentapharsodinium dalei*, MD95-2015-0 cm. (g) *Spiniferites mirabilis*, MD95-2015-1850 cm.

Alexandrium excavatum (Braarud 1945) Balech and Tangen 1985

Family: GONYAULACACEAE Lindeman, 1928

Ataxiodinium choane Reid 1974

Bitectatodinium tepikiense (Wilson, 1973)

Impagidinium aculeatum (Wall 1967) Lentin and William 1981

Impagidinium pallidum Bujak 1984

Impagidinium paradoxum (Wall 1967) Stover and Evitt 1978

Impagidinium patulum (Wall 1967) Stover and Evitt 1978

Impagidinium sphaericum (Wall 1967) Lentin and Williams 1981

Impagidinium strialatum (Clarke and Verdier 1967) Stover and Evitt 1978

Impagidinium spp. Indet. Stover and Evitt 1978

Lingulodinium machaerophorum (Deflandre and Cookson, 1955) Wall, 1967

Nematosphaeropsis labyrinthus (Ostenfeld, 1903) Reid, 1974

Operculodinium centrocarpum (Deflandre and Cookson, 1955) Wall, 1967

Operculodinium israelianum (Rossignol 1962) Wall 1967

Operculodinium janduchenei Head et al., 1989

Operculodinium short processes

Pyxidinopsis reticulata (McMinn and Sun 1994) Marret and de Vernal, 1997

Spiniferites bentorii (Rossignol 1964) Wall et Dale 1970

Spiniferites bulloideus (Deflandre and Cockson, 1955) Sarjeant, 1970

Spiniferites delicatus Reid 1974

Spiniferites elongatus Reid 1974

Spiniferites frigidus Harland and Reid, in Harland et al., 1980

Spiniferites lazus Reid 1974

Spiniferites membranaceus (Rossignol 1964) Sarjeant 1970

Spiniferites mirabilis (Rossignol 1964) Sarjeant 1970

Spiniferites ramosus (Ehrenberg 1838) Mantell 1854

Spiniferites pachyderma (Rossignol 1964) Reid 1974

Spiniferites spp. Indet. Mantell 1850

Order: PERIDINIALES Haeckel, 1894

Suborder PERIDINIINEAE (autonym)

Family CONGRUENTIDIACEAE Schiller 1935

Brigantedinium spp. Reid, 1977 (includes all the specimen of *Brigantedinium* species grouped because of crumpled aspect of the cysts)

Selenopemphix nephroides (Benedek, 1972) Bujak in Bujak et al., 1980, Benedek and Sargeant, 1981

Selenopemphix quanta (Bradford,1975) Harland, 1981: synonym: *Multispinula quanta*

Family PERIDINIACEAE Ehrenberg 1831

Pentapharsodinium dalei Indelicato et Loeblich III 1986

Family PROTOPERIDINIACEAE Balech, 1988 nom. cons.

Islandinium minutum (Harland and Reid in Harland et al., 1980) Head et al., 2001

Trinovantedinium applanatum Reid 1977 = *Protoperidinium pentagonum* (Gran 1902) Balech 1974

Peridinoid

Subclass GYMNODINIPHYCIDAE Fensome et al., 1993

Order GYMNODINIALES Apstein 1909

Family POLYKRIKACEAE Kofoid et Swezy 1921

Polykrikos schwartzii Bütschli 1873

References

Aksu, A.E., de Vernal, A., Mudie, P.J., 1989. High resolution foraminifer, palynologic, and stable isotopic records of upper Pleistocene sediments from the Labrador Sea: Paleoclimatic and paleoceanographic trends. Proc. ODP, Sci. Results 105, pp. 617–642.

Alley, R.B., Mayewski, P.A., Sowers, T., Stuiver, M., Taylor, K.C., Clark, P.U., 1997. Holocene climatic instability: A prominent, widespread event 8200 yr ago. Geology 25, 483–486.

Baldini, J.U.L., McDermott, F., Fairchild, I.J., 2002. Structure of the 8200-year cold event revealed by a speleothem trace element record. Science 296, 2203–2206.

Barber, D.C., Dyke, A., Hillaire-Marcel, C., Jennings, A.E., Andrews, J.T., Kerwin, M.W., Bilodeau, G., McNeely, R., Southon, J., Morehead, M.D., Gagnon, J.-M., 1999. Forcing of the cold event of 8200 years ago by catastrophic drainage of Laurentide lakes. Nature 400, 344–348.

Bard, E., 1998. Geochemical and geophysical implications of the radiocarbon calibration. Geochimica Cosmochimica Acta 62, 2025–2038.

Bassinot, F., Labeyrie, L., 1996. Les rapports de campagne à la mer à bord du Marion-Dufresne: Campagne IMAGES MD 101 (du 29-05-95 au 11-07-95). IFRTP Editions, Brest.

Boessenkool, K.P., Brinkhuis, H., Schonfeld, J., Targarona, J.U., 2001. North Atlantic sea-surface temperature changes and the climate of western Iberia during the last deglaciation; a marine palynological approach. Glob. Planet. Change 30, 33–39.

Bond, G., Showers, W., Cheseby, M., Lotti, R., Almasi, P., deMenocal, P., Priore, P., Cullen, H., Hajdas, I., Bonani, G., 1997. A pervasive millenial-scale cycle in North Atlantic Holocene and Glacial climates. Science 278, 1257–1266.

Broecker, W.S., Bond, G., Klas, M., 1990. A salt oscillator in the glacial Atlantic? 1. The concept. Paleoceanography 5, 469–477.

Cortijo, E., Duplessy, J.C., Labeyrie, L.D., Leclaire, H., Duprat, J., Van weering, T.C.E., 1994. Eemian cooling in the Norwegian Sea and North Atlantic Ocean preceding continental ice-sheet growth. Nature 372, 446–449.

Cortijo, E., Lehman, S., Keigwin, L., Chapman, M., Paillard, D., Labeyrie, L., 1999. Changes in meridional temperature and salinity gradients in the North Atlantic Ocean (30°–72°N) during the last interglacial period. Paleoceanography 14, 23–33.

Cortijo, E., Labeyrie, L., Elliot, M., Balbon, E., Tisnerat, N., 2000. Rapid climatic variability of the North Atlantic Ocean and global climate: A focus of the IMAGES program. Quat. Sci. Rev. 19, 227–241.

Dale, B., 1976. Cyst formation, sedimentation, and preservation: Factors affecting dinoflagellate assemblages in recent sediments from Trondheimsfjord, Norway. Rev. Palaeobot. Palynol. 22, 39–60.

Dale, B., 1996. Dinoflagellate cyst ecology: Modelling and geological applications. In: Jansonius, J., McGregor, D.C. (Eds.), Palynology: Principles and Applications. AASP Foundation, Dallas, TX, pp. 1249–1276.

Dean, W.E., Forester, R.M., Bradbury, J.P., 2002. Early Holocene change in atmospheric circulation in the Northern great plains: An upstream view of the 8.2 ka cold event. Quat. Sci. Rev. 21, 1763–1775.

de Vernal, A., Rochon, A., Hillaire-Marcel, C., Turon, J.-L., Guiot, J., 1993. Quantitative reconstruction of sea-surface conditions, seasonal extent of sea-ice cover and meltwater discharges in high latitude marine environments from dinoflagellate cyst assemblages. In: Peltier, W.R. (Ed.), Proceedings of the NATO Workshop on Ice in the Climate System. NATO ASI Series, Springer, Berlin, I12, pp. 611–621.

de Vernal, A., Henry, M., Bilodeau, G., 1996. Techniques de préparation et d'analyse en micropaléontologie. Les Cahiers du GEOTOP 3.

de Vernal, A., Rochon, A., Turon, J.-L., Matthiessen, J., 1997. Organic-walled dinoflagellate cysts: Palynological tracers of sea-surface conditions in middle to high latitude marine environments. Geobios 30, 905–920.

de Vernal, A., Hillaire-Marcel, C., 2000. Sea-ice cover, sea-surface salinity and halo-/thermocline structure of the northwest North Atlantic: Modern versus full glacial conditions. Quat. Sci. Rev. 19, 65–85.

de Vernal, A., Henry, M., Matthiessen, J., Mudie, P.J., Rochon, A., Boessenkool, K.P., Eynaud, F., Grøsfjeld, K., Guiot, J., Hamel, D., Harland, R., Head, M.J., Kunz-Pirrung, M., Levac, E., Loucheur, V., Peyron, O., Pospelova, V., Radi, T., Turon, J.-L., Voronina, E., 2001. Dinoflagellate cyst assemblages as tracers of sea-surface conditions in the northern North Atlantic, Arctic and sub-Arctic seas: The new '$n = 677$' data base and its application for quantitative palaeoceanographic reconstruction. J. Quat. Sci. 16, 681–698.

Devillers, R., de Vernal, A., 2000. Distribution of dinoflagellate cysts in surface sediments of the northern North Atlantic in relation to nutrient content and productivity in surface waters. Mar. Geol. 166, 103–124.

Eiríksson, J., Knudsen, K.L., Haflidason, H., Heinemeier, J., 2000. Chronology of late Holocene climatic events in the northern North Atlantic based on AMS 14C dates and tephra markers from the volcano Hekla, Iceland. J. Quat. Sci. 15, 573–580.

Eynaud, F., 1999. Kystes de dinoflagellés et evolution paléoclimatique et paléohydrologique de l'Atlantique Nord au cours du Dernier Cycle Climatique du Quaternaire. Ph.D. Thesis, Université Bordeaux I, Talence.

Eynaud, F., Turon, J.L., Sanchez-Goni, M.F., Gendreau, S., 2000. Dinoflagellate cyst evidence of 'Heinrich-like events' off Portugal during the Marine Isotopic Stage 5. Mar. Micropaleontol. 40, 9–21.

Eynaud, F., Turon, J.L., Matthiessen, J., Kissel, C., Peypouquet, J.P., de Vernal, A., Henry, M., 2002. Norwegian sea-surface palaeoenvironments of marine oxygen-isotope stage 3: The paradoxical response of dinoflagellate cysts. J. Quat. Sci. 17, 349–359.

Faugères, J.-C., Mézerais, M.L., Stow, D.A.V., 1993. Contourite drift types and their distribution in the North and South Atlantic Ocean basins. Sediment. Geol. 82, 189–203.

Faugères, J.-C., Stow, D.A.V., Imbert, P., Viana, A., 1999. Seismic features diagnostic of contourite drifts. Mar. Geol. 162, 1–38.

Forsstrom, L., 2001. Duration of interglacials: A controversial question. Quat. Sci. Rev. 20, 1577–1586.

Gajewski, K., Vance, R., Sawada, M., Fung, I., Gignac, L.D., Halsey, L., John, J., Maisongrande, P., Mandell, P., Mudie, P., Richard, P., Sherrin, A.G., Soroko, J., Vitt, D., 2000. The climate of North America and adjacent ocean waters ca. 6 ka. Can. J. Earth Sci. 37.

Giraudeau, J., Cremer, M., Manthe, S., Labeyrie, L., Bond, G., 2000. Coccolith evidence for instabilities in surface circulation south of Iceland during Holocene times. Earth Planet. Sci. Lett. 179, 257–268.

GRIP members, 1993. Climate instability during the last interglacial period recorded in the GRIP ice core. Nature 364, 203–207.

Grootes, P.M., Stuiver, M., White, J.W.C., Johnsen, S.J., Jouzel, J., 1993. Comparison of oxygen isotope records from the GISP2 and GRIP Greenland ice cores. Nature 366, 552–554.

Grootes, P.M., Stuiver, M., 1997. Oxygen 18/16 variability in Greenland snow and ice with 10^3 to 10^5-year time resolution. J. Geophys. Res. 102, 26455–26470.

Guiot, J., 1990. Methodology of the last climatic cycle reconstruction in France from pollen data. Palaeogeogr. Palaeoclimatol. Palaeoecol. 80, 49–69.

Guiot, J., Goeury, C., 1996. PPPbase, a software for statistical analysis of paleoecological data. Dendrochronologia 14, 295–300.

Harland, R., 1983. Distribution maps of recent dinoflagellate cysts in bottom sediments from the North Atlantic Ocean and adjacent seas. Paleontology 26, 321–387.

Harland, R., Howe, J.A., 1995. Dinoflagellate cysts and Holocene oceanography of the northeastern Atlantic Ocean. Holocene 5, 220–228.

Head, M.J., Harland, R., Matthiessen, J., 2001. Cold marine indicators of the late Quaternary: The new dinoflagellate cyst genus *Islandinium* and related morphotypes. J. Quat. Sci. 16, 621–636.

Jansen, E., Bjørklund, K.R., 1985. Surface ocean circulation in the Norwegian Sea 15,000 B.P. to present. Boreas 14, 243–257.

Johnsen, S.J., Clausen, H.B., Dansgaard, W., Gundestrup, N.S., Hammer, C.U., Tauber, H., 1995. The Eem stable isotope record along the GRIP Ice Core and its Interpretation. Quat. Res. 43, 117–124.

Karlin, R., Lyle, M., Zahn, R., 1992. Carbonate variations in the North-east Pacific during the late Quaternary. Paleoceanography 7, 43–61.

Kissel, C., Laj, C., Mazaud, A., Dokken, A., 1998. Magnetic anisotropy and environmental changes in two sedimentary cores from the Norwegian Sea and the North Atlantic. Earth Planet. Sci. Lett. 164, 617–626.

Kissel, C., Laj, C., Labeyrie, L., Dokken, T., Voelker, A., Blamart, D., 1999. Rapid climatic variations during Marine Isotopic Stage 3: Magnetic analysis of sediments from Nordic Seas and North Atlantic. Earth Planet. Sci. Lett. 171, 489–502.

Klitgaard-Kristensen, D., Sejrup, H.P., Haflidason, H., Johnsen, S., Spurk, M., 1998. A regional 8200 cal. yr BP cooling event in northwest Europe, induced by final stages of the Laurentide ice-sheet deglaciation? J. Quat. Sci. 13, 165–169.

Knudsen, K.L., Eiriksson, J., 2002. Application of tephrochronology to the timing and correlation of palaeoceanographic events recorded in Holocene and Late Glacial shelf sediments off North Iceland. Mar. Geol. 191, 165–188.

Koç, N., Jansen, E., Hald, M., Labeyrie, L., 1996. Late glacial–Holocene sea surface temperatures and gradients between the North Atlantic and the Norwegian Sea: Implication for the Nordic heat pump. In: Andrews, J.T., Austin, W.E.N., Bergsten, H., Jennings, E. (Eds.), Late Quaternary Paleoceanography of the North Atlantic Margins. Geol. Soc. Spec. Publ., London, pp. 177–185.

Kukla, G.J., Bender, M.L., de Beaulieu, J.-L., Bond, G., Broecker, W.S., Cleveringa, P., Gavin, J.E., Herbert, T.D., Imbrie, J., Jouzel, J., 2002. Last Interglacial Climates. Quat. Res. 58, 2–13.

Leuenberger, M.C., Lang, C., Schwander, J., 1999. Delta N measurements as a calibration tool for the paleothermometer and gas-ice age differences: A case study for the 8200 B.P. event on GRIP ice. J. Geophys. Res. 104, 22,163–22,170.

Loutre, M.F., Berger, A., 2003. Marine Isotope Stage 11 as an analogue for the present interglacial. Glob. Planet. Change 36, 209–217.

Mangin, S., 2002. Distribution actuelle des kystes de dinoflagellés en méditerranée occidentale et application aux fonctions de transfert. M.Sc. Thesis, Université Bordeaux I, Talence.

Manthé, S., 1998. Variabilité de la circulation thermohaline glaciaire et interglaciaire en Atlantique Nord, tracée par les foraminifères planctoniques et la microfaune benthique. Ph.D. Thesis, Université Bordeaux I, Talence.

Marchal, O., Cacho, I., Stocker, T.F., Grimalt, J.O., Calvo, E., Martrat, B., Shackleton, N., Vautravers, M., Cortijo, E., van Kreveld, S., 2002. Apparent long-term cooling of the sea surface in the northeast Atlantic and Mediterranean during the Holocene. Quat. Sci. Rev. 21, 455–483.

Marret, F., Turon, J.-L., 1994. Paleohydrology and paleoclimatology off Northwest Africa during the last glacial–interglacial transition and the Holocene: Palynological evidences. Mar. Geol. 118, 107–117.

Martinson, D.G., Pisias, N.G., Hays, J.D., Imbrie, J., Moore, T.C., Shackleton, N.J., 1987. Age dating and the orbital theory of the ICE Ages: Development of a high resolution 0 to 300,000 year chronostratigraphy. Quat. Res. 27, 1–29.

Maslin, M., Sarnthein, M., Knaack, J.-J., Grootes, P., Tzedakis, C., 1998. Intra–interglacial cold events: An Eemian–Holocene comparison. In: Cramp, A., MacLeod, C.J., Lee, S.V., Jones, E.J.W. (Eds.), Geological Evolution of Ocean Basins. Results from the Ocean Drilling Program, London, pp. 91–99.

Matthiessen, Y., 1995. Distribution patterns of dinoflagellate cysts and other organic-walled microfossils in Recent Norwegian–Greenland Sea sediments. Mar. Micropaleontol. 24, 307–334.

Matthiessen, J., Knies, J., 2001. Dinoflagellate cyst evidence for warm interglacial conditions at the northern Barents Sea margin during marine oxygen isotope stage 5. J. Quat. Sci. 16, 727–737.

McManus, J.F., Oppo, D.W., Keigwin, L.D., Cullen, J.L., Bond, G.C., 2002. Thermohaline circulation and prolonged interglacial warmth in the North Atlantic. Quat. Res. 58, 17–21.

Meese, D.A., Alley, R.B., Fiacco, R.J., Germani, M.S., Gow, A.J., Grootes, P.M., Illing, M., Mayewski, P.A., Morrison, M.C., Ram, M., Taylor, K.C., Yang, Q., Zielinski, G.A., 1994. Preliminary Depth–Age Scale of the GISP2 Ice Core. Special CRREL Report 94-1.

Morzadec-Kerfourn, M.-T., 1992. Upper Pleistocene and Holocene dinoflagellate cyst assemblages in marine environments of the Mediterranean Sea and the northwest Atlantic Coast of France. In: Head, M.J., Wrenn, H. (Eds.), Neogene and Quaternary Dinoflagellate Cyst of the North Atlantic Ocean and Adjacent Seas: Ecostratigraphy and Biostratigraphy. AASP Foundation, Dallas, TX, pp. 121–132.

Nesje, A., Dahl, S.O., 2001. The Greenland 8200 cal. yr BP event detected in loss-on-ignition profiles in Norwegian lacustrine sediment sequences. J. Quat. Sci. 16, 155–166.

NODC, 1994. NODC (Levitus) World Ocean Atlas 1994 data provided by the NOAA-CIRES Climate Diagnostics Center, Boulder, Colorado, USA, from their Web site at http://www.cdc.noaa.gov/

Orvik, K.A., Skagseth, O., Mork, M., 2001. Atlantic inflow to the Nordic Seas: Current structure and volume fluxes from moored current meters, VM-ADCP and SeaSoar-CTD observations, 1995–1999. Deep-Sea Res. I 48, 937–957.

Poore, R.Z., Dowsett, H.J., 2001. Pleistocene reduction of polar ice-caps: Evidence from Cariaco Basin marine sediments. Geology 29, 71–74.

Revel, M., Cremer, M., Grousset, F.E., Labeyrie, L., 1996. Grain-size and Sr–Nd isotopes as tracer of paleo-bottom current strength, Northeast Atlantic Ocean. Mar. Geol. 131, 233–249.

Rochon, A., de Vernal, A., Sejrup, H.-P., Haflidason, H., 1998. Palynological evidence of climatic and oceanographic changes in the North Sea during the last deglaciation. Quat. Res. 49, 197–207.

Rochon, A., de Vernal, A., Turon, J.-L., Matthiessen, J., Head, M.J., 1999. Recent dinoflagellate cysts of the North Atlantic Ocean and adjacent seas in relation to sea-surface parameters. Am. Assoc. Stratigr. Palynol. Contrib. Ser. 35.

Sanchez-Goñi, M.F., Eynaud, F., Turon, J.L., Shackleton, N.J., 1999. High resolution palynological record off the Iberian margin: Direct land–sea correlation for the Last Interglacial complex. Earth Planet. Sci. Lett. 171, 123–137.

Sánchez-Goñi, M.-F., Turon, J.-L., Eynaud, F., Shackleton, N.J., Cayre, O., 2000. Direct land–sea correlation of the Eemian, and its comparison with the Holocene: A high resolution palynological record off the Iberian margin. Neth. J. Geosci. 79, 345–354.

Sarnthein, M., Tiedemann, R., 1990. Younger Dryas-style cooling events at Glacial terminations I–VI at ODP Site 658: Associated benthic $\delta^{13}C$ anomalies constrain meltwater hypothesis. Paleoceanography 5, 1041–1055.

Seidenkrantz, M.S., 1993. Benthic foraminiferal and stable isotope evidence for a 'Younger Dryas-style' cold spell at the Saalian–Eemian transition, Denmark. Palaeogeogr. Palaeoclimatol. Palaeoecol. 102, 103–120.

Shackleton, N.J., Chapman, M., Sanchez-Goni, M.F., Pailler, D., Lancelot, Y., 2002. The Classic Marine Isotope Substage 5e. Quat. Res. 58, 14–16.

Steig, E.J., Grootes, P.M., Stuiver, M., 1994. Seasonal precipitation timing and ice core records. Science 266, 1885–1886.

Stoner, J.S., Laj, C., Channell, J.E.T., Kissel, C., 2002. South Atlantic and North Atlantic geomagnetic paleointensity stacks (0–80 ka): Implications for inter-hemispheric correlation. Quat. Sci. Rev. 21, 1141–1151.

Stuiver, M., Grootes, P.M., Braziunas, T.F., 1995. The GISP2 ^{18}O climate record of the past 16,500 years and the role of the sun, ocean and volcanoes. Quat. Res. 44, 341–354.

Stuiver, M., Reimer, P.J., Bard, E., Beck, J.W., Burr, G.S., Hughen, K.A., Kromer, B., McCormac, G., van der Plicht, J., Spurk, M., 1998. INTCAL98 Radiocarbon Age Calibration, 24,000–0 cal BP. Radiocarbon 40, 1041–1083.

Thouveny, N., de Beaulieu, J.-L., Bonifay, E., Creer, K.M., Guiot, J., Icole, M., Johnsen, S., Jouzel, J., Reille, M., Williams, T., Williamson, D., 1994. Climate variations in Europe over the past 140 kyr deduced from rock magnetism. Nature 371, 503–506.

Tomczak, M., Godfrey, J.S., 1994. Regional Oceanography: An Introduction. Pergamon, Oxford.

Turon, J.-L., 1978. Les dinoflagellés témoins des paléoenvironnements durant l'Holocène dans l'Atlantique Nord Oriental. Signification paléohydrologique et paléoclimatique. C.R. Acad. Sc. Paris 286, 1861–1864.

Turon, J.-L., 1981. Les kystes de dinoflagellés dans les sédiments récents de l'Atlantique Nord-oriental et leurs relations avec l'environnement océanique. Application aux dépôts holocènes du Chenal de Rockall. Mém. Mus. Natl. Hist. 27, 269–282.

Turon, J.-L., 1984. Le palynoplancton dans l'environnement actuel de l'Atlantique Nord-oriental. Evolution climatique et hydrologique depuis le dernier maximum glaciaire. Mém. Inst. Géol. Bassin d'Aquitaine 17.

Turon, J.-L., Londeix, L., 1988. Les asssemblages de kystes de dinoflagellés en Méditerranée occidentale (Mer d'Alboran): mise en évidence de l'évolution des paléoenvironnement depuis le dernier maximum glaciaire. Bull. Centr. Rech. Explor.-Prod. Elf–Aquitaine 12, 313–344.

Turon, J.-L., Lezine, A.-M., Denefle, M., in press. Land–sea correlations for the last glaciation inferred from a pollen and dinocyst record from the Portuguese margin. Quat. Res.

Versteegh, G.J.M., 1994. Recognition of cyclic and non-cyclic environmental changes in the Mediterranean Pliocene: A palynological approach. Mar. Micropaleontol. 23, 147–171.

von Grafenstein, U., Erlenkeuser, H., Muller, J., Jouzel, J., Johnsen, S., 1998. The cold event 8200 years ago documented in oxygen isotope records of precipitation in Europe and Greenland. Clim. Dynam. 14, 73–81.

Wall, D., Dale, B., Lohman, G.P., Smith, W.K., 1977. The environmental and climatic distribution of dinoflagellate cysts in modern marine sediments from regions in the North and south Atlantic oceans and adjacent seas. Mar. Micropaleontol. 2, 121–200.

Williams, D.B., 1971. The distribution of marine dinoflagellates in relation to physical and chemical conditions. In: Funnel, B.M., Riedel, R. (Eds.), The Micropaleoentology of the Oceans. Cambridge University Press, pp. 91–95.

Williams, G.L., Lentin, J.K., Fensome, R.A., 1998. The Lentin and Williams Index of Fossil Dinoflagellates: 1998 Edition. AASP Contrib. Ser. 34.

Yu, Z., Wright, H.E., Jr., 2001. Response of interior North

America to abrupt climate oscillations in the North Atlantic region during the last deglaciation. Earth-Sci. Rev. 52, 333–369.

Zonneveld, K.A.F., 1995. Palaeoclimatic and palaeo-ecological changes during the last deglaciation in the Eastern Mediterranean – implications for dinoflagellate ecology. Rev. Palaeobot. Palynol. 84, 221–253.

Zonneveld, K., Versteegh, G.J.M., de Lange, G.J., 1997. Preservation of organic walled dinoflagellate cysts in different oxygen regimes: A 10,000 Year natural experiment. Mar. Micropaleontol. 29, 393–405.

Zonneveld, K.A.F., Versteegh, G.J.M., de Lange, G.J., 2001. Palaeoproductivity and post-depositional aerobic organic matter decay reflected by dinoflagellate cyst assemblages of the Eastern Mediterranean S1 sapropel. Mar. Geol. 172, 181–195.